Microtubule Transport and Assembly during Axon Growth

Wenqian Yu, Matthew J. Schwei, and Peter W. Baas

Department of Anatomy, University of Wisconsin Medical School, Madison, Wisconsin 53706

Abstract. There is controversy concerning the mechanisms by which the axonal microtubule (MT) array is elaborated, with some models focusing on MT assembly and other models focusing on MT transport. We have proposed a composite model in which MT assembly and transport are both important (Joshi, H.C., and P.W. Baas. 1993. *J. Cell Biol.* 121:1191–1196). In the present study, we have taken a novel approach to evaluate the merits of this proposal. Biotinylated tubulin was microinjected into cultured neurons that had already grown short axons. The axons were then permitted to grow longer, after which the cells were prepared for immunoelectron microscopic analyses. We reasoned that any polymer that assembled or turned over subunits after the introduction of the probe should label for biotin, while any polymer that was already assembled but did not turnover should not label. Therefore, the presence in the newly grown region of the axon of any unlabeled MT polymer is indicative of MT transport. In sampled regions, the majority of the polymer was labeled, indicating that MT assembly events are active during axon growth. Varying amounts of unlabeled polymer were also present in the newly grown regions, indicating that MT transport also occurs. Together these findings demonstrate that MT assembly and transport both contribute to the elaboration of the axonal MT array.

T HERE is widespread agreement that the net addition of new microtubule (MT)[1] polymer to the axon is necessary for its growth, but there is controversy concerning the mechanisms by which this occurs. The earliest model, sometimes referred to as the structural hypothesis, held that preassembled MTs are transported from the cell body of the neuron down the growing axon (Lasek, 1986). A subsequent model, sometimes referred to as the distal assembly model, held that new polymer is added at the distal region of the growing axon via local MT assembly (Bamburg et al., 1986). Since these early models were proposed, many workers have taken the perspective that MT transport and assembly events are mutually exclusive, and hence that evidence supporting one model refutes the other. We have taken a very different perspective, that MT transport and assembly are both important during axon growth. In our model, MT transport is required to increase the tubulin levels within the axon, and local assembly events are required to regulate the lengths of the MTs (Joshi and Baas, 1993; Baas and Yu, 1996).

The most controversial element of our model is that it, like the earlier structural hypothesis, hinges on the movement of assembled MTs. Attempts to visualize MT transport down the axon using live-cell light microscopic methods have produced mixed and principally negative results (for example, see Okabe and Hirokawa, 1989; Lim et al., 1990; Takeda et al., 1995; Sabry et al., 1995), leading some authors to conclude that all of the MTs in the axon are stationary. These results have led to the speculation that tubulin may be actively transported down the axon not as polymer, but in another form such as free subunits or oligomers. It is also possible, however, that the movement of MTs down the axon occurs but is difficult to detect for technical reasons. For example, only a small fraction of the MTs may be moving at one time, and the movement of these MTs may be highly asynchronous. In addition, the movement of these MTs may be obscured by the fact that they are undergoing dynamic assembly events at the same time that they are moving. In support of this latter point, indirect but strong evidence for MT transport has been obtained in studies in which pharmacologic agents were used to suppress MT dynamics in the neuron (Baas and Ahmad, 1993; Smith, 1994; Ahmad and Baas, 1995; Yu and Baas, 1995).

These considerations suggest that MT transport probably occurs within the axon, but that higher resolution methods may be required to reveal this transport under normal conditions. In the present study, we have developed a novel strategy that does not rely on pharmacologic agents and that reveals the contributions of both MT transport and assembly. In this strategy, biotinylated tubulin is microinjected into cultured neurons after the out-

---

---

1. *Abbreviations used in this paper:* DIC, differential interference contrast; MT, microtubule.

growth of short axons. The axons are then permitted to grow longer, after which the cells are prepared for immunoelectron microscopic visualization of biotinylated tubulin–containing polymer. We reasoned that any polymer that assembled after the introduction of the probe should label for biotin, while any polymer that was already assembled but did not undergo assembly or subunit turnover should not label. Therefore, the presence in the newly grown region of the axon of any unlabeled MT polymer indicates that this polymer was transported during axon growth. Thus, using this technique, we are able to test our proposal that MT transport and assembly events both occur during axon growth.

Materials and Methods

Cell Culture

Cultures of rat sympathetic neurons were prepared as previously described (Baas and Ahmad, 1993). The cells were plated onto "special dishes" that were prepared by adhering a glass coverslip to the bottom of a 35-mm plastic petri dish into which had been drilled a 1-cm-diam hole. To ease the task of relocating cells of interest, we used coverslips that had been photoetched with demarcating boxes (Bellco Glass, Inc., Vineland, NJ). Before plating the cells, the glass-bottomed well of the special dish was treated with polylysine and laminin as previously described (Baas and Ahmad, 1993).

Experimental Regime

After plating, the neuron cultures were placed in an incubator for 2–3 h to permit the cells to adhere to the substratum and to extend axons. At this point, after which most of the neurons had extended multiple axons that were 25–100 μm in length, cultures were placed on the prewarmed stage of an inverted microscope (Axiovert 135M; Carl Zeiss, Inc., Thornwood, NY) equipped with an environmental chamber that effectively maintains temperature at 37°C. For microinjection, we selected neurons whose axons were not extensively branched and were clearly not fasciculated with the axons of neighboring cells. A phase-contrast or differential interference contrast (DIC) image of the entire neuron was obtained using a thermal video printer (Sony, Japan) either just before or just after microinjection. Biotinylated tubulin was prepared essentially as described by Webster and Borisy (1989) except that the final product was suspended at 4 mg/ml in an injection buffer containing 50 mM potassium glutamate and 1 mM MgCl₂, pH 6.8 (Schulze and Kirschner, 1986). Biotinylated tubulin was kept at 4°C until the time of injection and introduced into the neurons using the Eppendorf microinjection system (Eppendorf, Hamburg, Germany) at a volume roughly but not exceeding 10% of the volume of the cell. The culture was then returned to the incubator for 35 min to permit the axons to continue growing, after which a second set of phase-contrast or DIC images was obtained. The two sets of images were subsequently used to assess the degree to which individual axons had grown during the 40-min period of time postinjection.

Immunofluorescence and Immunoelectron Microscopy

Immediately after acquiring the second set of phase-contrast or DIC images, the cultures were extracted for 7 min in a MT stabilizing buffer (60 mM Pipes, 25 mM Hepes, 10 mM EGTA, 2 mM MgCl₂, 10 μM taxol, pH 6.9) containing 0.5% Triton X-100 to remove unassembled tubulin. The cultures were then fixed by the addition of an equal quantity of the buffer containing 1% glutaraldehyde. After 10 min of fixation, the cultures were rinsed in buffer and incubated for 15 min in 3 mg/ml sodium borohydride (dissolved in half buffer and half methanol to reduce bubbling), incubated for 30 min in a blocking solution containing 5% normal goat serum and 2% BSA in TBS-1 (10 mM Tris, 140 mM NaCl, pH 7.6), and then exposed to primary antibody overnight at 4°C. The primary antibody was a mouse monoclonal anti-biotin antibody conjugated directly to the fluorochrome Cy-3 (Jackson Immunoresearch Laboratories, West Grove, PA) and was used at a concentration of 1:50. After incubation with the primary antibody, the cultures were rinsed six times for 10 min each with TBS-2 (20 mM Tris, 140 mM NaCl, pH 8.2) containing 0.1% BSA, visualized, and

photographed using epifluorescence optics on the Axiovert microscope. The cultures were then incubated for 3 h at 37°C with an appropriate second antibody conjugated to 5-nm colloidal gold particles. The gold-conjugated second antibody was purchased from Amersham Corp. (Arlington Heights, IL) and used at a concentration of 1:2. After incubation with the second antibody, the cultures were rinsed six times in TBS-2, fixed in 2% glutaraldehyde in 0.1 M cacodylate also containing 0.2% tannic acid, rinsed in 0.1 M cacodylate, postfixed for 10 min in 2% osmium tetroxide in 0.1 M cacodylate, dehydrated in an ethanol series, and embedded in LX100 (Ladd Research Industries, Inc., Burlington, VT). After curing of the resin, the glass coverslip was dissolved from the resin by a 10-min incubation in hydrofluoric acid. Cells of interest were relocated using the video images and the photoetched pattern transferred from the glass coverslip onto the resin, circled with a diamond-marker objective, and thin sectioned using an ultramicrotome (Ultracut E; Reichert-Jung, Vienna). The sections were picked up onto formvar-coated slot grids, stained with uranyl acetate and lead citrate, and viewed with a transmission electron microscope (CX100; JEOL USA Inc., Peabody, MA).

Data Analysis

All sections through the injected neurons were viewed, and a typical middle section was used for quantification of labeled and unlabeled MT polymer. Distinguishing labeled and unlabeled polymer was difficult in some areas along the length of the axon because the tight spacing of the MTs made it impossible to know the correct MT with which many of the gold particles were associated. In other areas in which the MTs were even more tightly bundled, there was some suspicion that polymer may not have labeled due to problems of accessibility of the gold particles. To avoid misinterpretations, we used for our analyses only areas of the axons in which the MTs had splayed apart sufficiently during extraction to minimize these potential problems. We uniformly selected (as indices of total labeled and unlabeled polymer levels) areas of the axon that were 4 μm in length and scored total lengths of labeled and unlabeled MT polymer within these regions. These data were then expressed as a percentage of unlabeled polymer on a composite schematic figure. Selected areas for analysis included both the newly grown region of the axon as well as other points along its length.

Results

Experimental Regime

Fig. 1 schematically illustrates our strategy for studying MT transport and assembly during axon growth. Rat sympathetic neurons were grown on a laminin substratum to promote rapid axon outgrowth. 2 h after plating, by which time axons had grown to be 25–100 μm in length, biotinylated tubulin was microinjected into the cell body of the neuron. The biotinylated tubulin rapidly intermingles with native tubulin and diffuses down axons of this length (with the assistance of the pressure of injection) within 1–2 min of injection (see Okabe and Hirokawa, 1988; Li and Black, 1996). We reasoned that any MT polymer that assembles or turns over after the introduction of the biotinylated tubulin should incorporate the probe and hence label for biotin in immunomicroscopic assays. If MT assembly but not transport supplies new polymer for the newly grown region of the axon, then this region should contain exclusively labeled polymer. On the other hand, if MTs are transported into the newly grown region, then we should be able to detect unlabeled polymer in this region. Notably, we would expect MT assembly dynamics, including normal turnover or exchange of tubulin subunits with the unassembled tubulin pool, to accompany MT transport events. Therefore, the fact that polymer is labeled for biotin does not indicate that it was not transported, only that dynamic events occurred more rapidly than the polymer may or may not have been transported. Given that much
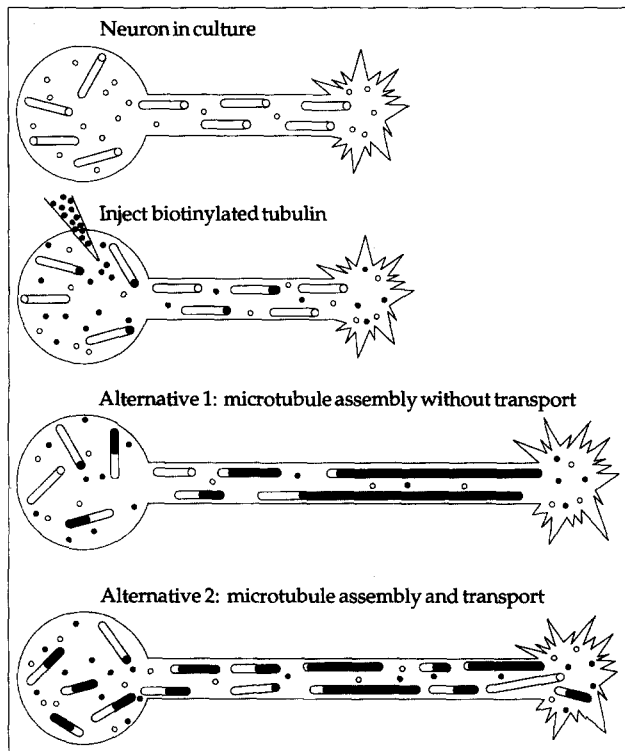
Figure 1. Schematic illustration of our experimental strategy. Native MTs and free tubulin are shown by unblackened tubes and circles, respectively. Biotinylated tubulin and regions of MTs containing biotinylated tubulin are shown in black. See Results for details.

Figure 2. Introduction and incorporation of biotinylated tubulin in the MTs of a cultured neuron. a shows a phase-contrast image of a typical neuron immediately after injection of biotinylated tubulin, while b shows that the axons have elongated after 40 min. c is the immunofluorescence image of the same neuron stained for biotin, showing incorporation of the probe into MTs (note fibrous appearance of staining in some areas where the bundled MTs splay apart). d–f show comparable images of another neuron with axons that grew somewhat more extensively over the 40-min period of time. Bar, 20 μm.

of the polymer turns over quite rapidly, particularly that extending into the distal region of the axon (see Ahmad et al., 1993), it was necessary that we focus on relatively short time points postinjection. For this reason, we chose a time of 40 min postinjection after which we extracted in a MT-stabilizing buffer, fixed, and prepared cultures for immunomicroscopic visualization of biotinylated tubulin–containing polymer (see Materials and Methods).

Fig. 2, a–f, shows images of two different neurons immediately after injection of biotinylated tubulin (Fig. 2, a and d), after 40 min of axon elongation (Fig. 2, b and e), and after preparation for immunofluorescence visualization of biotinylated tubulin–containing MTs (Fig. 2, c and f). A total of 19 axons grown from nine different neurons were analyzed. The average length of the axons at the time of injection was 60.2 ± 12.9 μm, while the average amount of growth per axon was 17.5 ± 6.1 μm. These rates of growth were generally similar to the rates at which the axons of uninjected neurons grew, typically 20–50 μm/h, indicating that the injection procedure did not markedly alter the growth properties of the axons. The immunofluorescence images in Fig. 2, c and f, show that the probe has incorporated into MTs.

Immunoelectron Microscopic Analyses

To quantify the levels of polymer that did or did not incorporate biotinylated tubulin, we took advantage of the high degree of resolution afforded by immunoelectron microscopy. This method has been effective in discerning newly
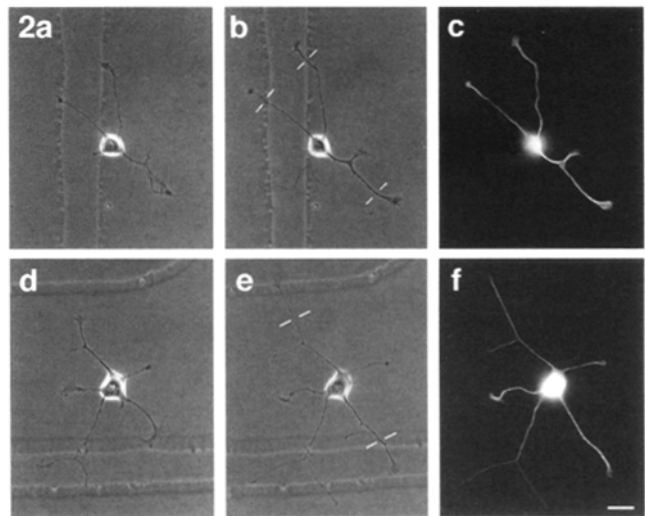
assembled from older regions of MTs in several previous studies (Okabe and Hirokawa, 1988; Baas and Black, 1990; Baas and Ahmad, 1992; Ahmad et al., 1993). Nevertheless, we used extra caution in selecting discrete regions of the axon (4 μm in length) in which the MTs splayed apart sufficiently during extraction so that there was minimal ambiguity in our identification of labeled and unlabeled polymer (see Materials and Methods). The total lengths of unlabeled and labeled polymer in these regions were scored. The percentage of unlabeled polymer in the selected regions was then taken as an index of the total percentage of unlabeled polymer. The density of gold particles on the labeled polymer (20–30 particles per μm of polymer) was generally similar throughout an individual neuron and among different injected neurons, confirming that we were relatively consistent in the levels of probe that we introduced into each cell, and that the probe rapidly diffused throughout the cell. Figs. 3, 4, and 5 show results obtained from three different axons, and the data for all 19 axons are shown schematically in Fig. 6.

Fig. 3, a and b, respectively, are tracings obtained from the DIC videoprint images of an entire neuron immediately after injection and 40 min later. The remaining panels show immunoelectron micrographs from the cell body (Fig. 3 c) and designated sites along the length of one of the axons as indicated in Fig. 3 b. This axon was 55 μm in length before injection and grew an additional 11 μm after injection. The cell body of this neuron and all other neurons examined contained both labeled and unlabeled polymer as did all regions of the axon proximal to the newly grown region. Fig. 3 d shows a site proximal to the newly grown region in which 33% of the polymer was unlabeled. In the case of this axon, almost all of the polymer in the
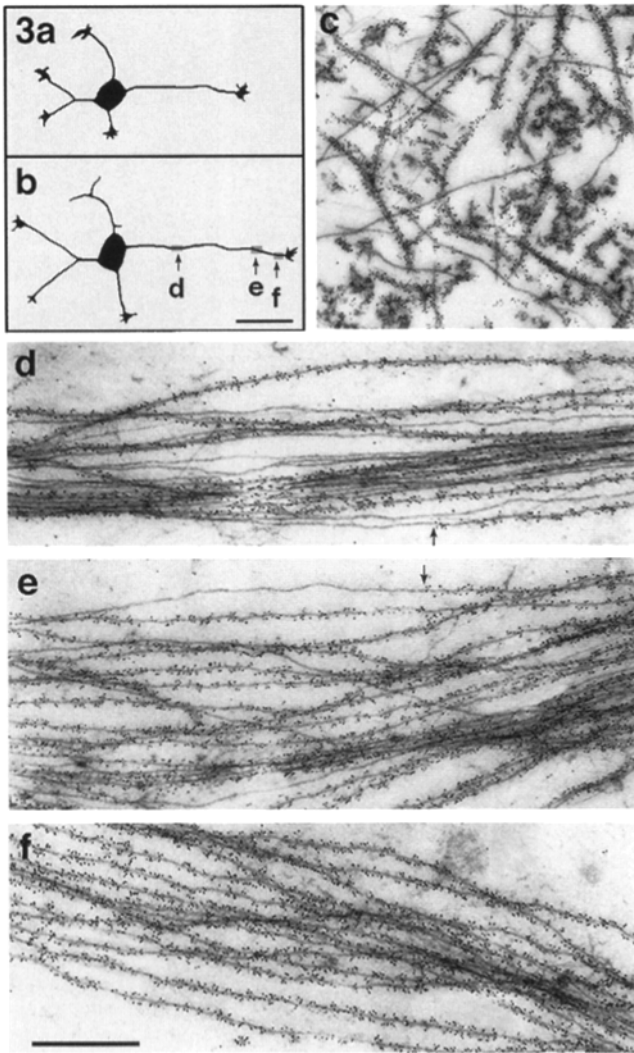
Figure 3. Immunoelectron microscopic visualization of MT polymer that did or did not incorporate biotinylated tubulin. *a* and *b*, respectively, are tracings obtained from the DIC videoprint images of an entire neuron immediately after injection and 40 min later. The remaining panels show immunoelectron micrographs from the cell body (*c*), and designated sites along the length of one of the axons as indicated in *b*. The cell body contains both labeled and unlabeled polymer as do all regions of the axon proximal to the newly grown region. *d* shows a site proximal to the newly grown region in which 33% of the polymer was unlabeled. *e* shows a fairly proximal site within the newly grown region in which a few unlabeled MT profiles intermingle with many labeled profiles. 10% of the polymer is unlabeled. Arrows on *d* and *e*, points where labeled and unlabeled polymer are continuous with one another, with the former elongating from the plus end of the latter. *f*, a distal site near the growth cone in which all of the polymer was labeled. Bars: (*a* and *b*) 20 μm; (*c–f*) 1.0 μm.

Figure 4. Immunoelectron microscopic visualization of MT polymer that did or did not incorporate biotinylated tubulin. *a* and *b*, respectively, are tracings obtained from the DIC videoprint images of a neuron immediately after injection and 40 min later. The remaining panels show immunoelectron micrographs from two different sites along one of the axons. *c* is a site proximal to the newly grown region in which 35% of the polymer was unlabeled. *d* is a site within the newly grown region in which 27% of the polymer was unlabeled. Notably, this site was located within the most distal region of the axon, directly behind the growth cone, a site that contained no unlabeled polymer in the axon shown in Fig. 3. Bars: (*a* and *b*) 20 μm; (*c* and *d*) 0.5 μm.

newly grown region was labeled. Fig. 3 *e* shows a fairly proximal site within the newly grown region in which a few unlabeled MT profiles intermingle with many labeled profiles. At this particular site, 10% of the polymer was unlabeled. Examination of serial sections indicated that labeled and unlabeled polymer were continuous with one another, with the former elongating from the plus end of
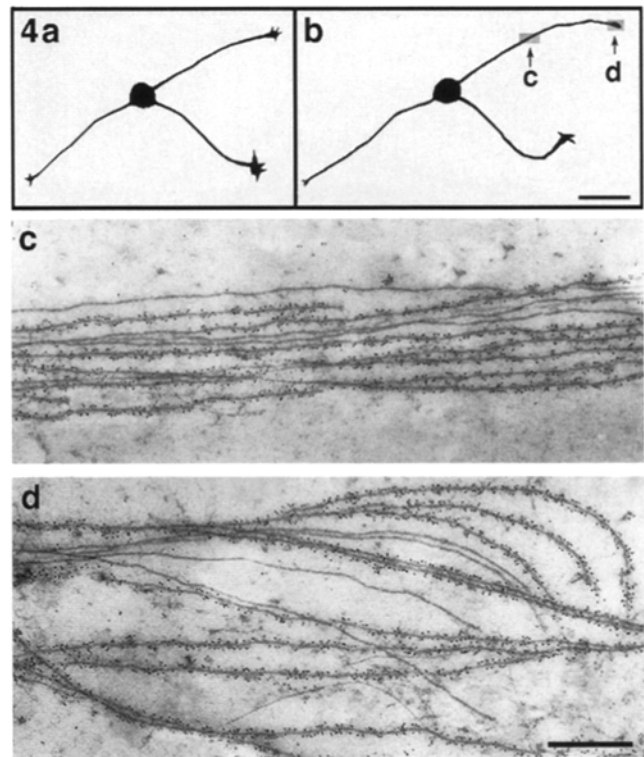
the latter (see also Okabe and Hirokawa, 1988). In no case did we observe unlabeled polymer extending from the plus end of labeled polymer (see also Okabe and Hirokawa, 1988; Li and Black, 1996). This was also apparent in many of the individual sections (see *arrows* on Fig. 3, *d* and *e*). Beyond this proximal area of the newly grown region, all of the MT profiles were labeled (Fig. 3 *f*). The fact that we were able to detect unlabeled polymer, even at these relatively low levels, indicates that MTs were transported into the newly grown region of the axon.

Fig. 4, *a* and *b*, respectively, are tracings obtained from the DIC videoprint images of another neuron immediately after injection and 40 min later. The remaining panels show immunoelectron micrographs from two different sites along one of the axons. This axon was 62 μm in length before injection and grew an additional 10 μm after injection. Fig. 4 *c* is a site proximal to the newly grown region in which 35% of the polymer was unlabeled. Fig. 4 *d* is a site within the newly grown region in which 27% of the polymer was unlabeled. Notably, this site was located within the most distal region of the axon, directly behind the growth cone, a site that contained no unlabeled poly-
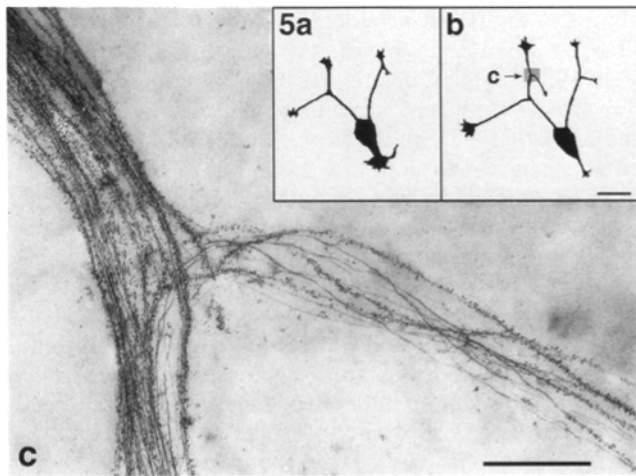
Figure 5. Immunoelectron microscopic visualization of MT polymer that did or did not incorporate biotinylated tubulin. *a* and *b*, respectively, are tracings obtained from the DIC videoprint images of a third neuron immediately after injection and 40 min later. During the 40-min time frame of the experiment, the growth cone at the tip of one of the axons underwent an asymmetric bifurcation. The larger branch grew straight, while the smaller branch curved off in another direction. *c* is an immunoelectron micrograph showing the region of the parent axon contiguous with both branches. In the region of the parent axon just proximal to the branch point, 19% of the polymer is unlabeled. In the larger branch, virtually all of the polymer is labeled. In regions along the length of the smaller branch, 40–50% of the polymer is unlabeled. Bars: (*a* and *b*) 20 μm; (*c*) 1.0 μm.

mer in the axon shown in Fig. 3. These data indicate that MTs were transported into the newly grown region of this axon, and together with the data from Fig. 3, show that MT transport is more apparent in some axons than in others.

Fig. 5, *a* and *b*, respectively, are tracings obtained from the DIC videoprint images of a third neuron immediately after injection and 40 min later. During the 40-min time frame of the experiment, the growth cone at the tip of one of the axons underwent an asymmetric bifurcation. The larger branch grew straight and was essentially a continuation of the parent axon, while the smaller branch curved off in another direction. Fig. 5 *c* is an immunoelectron micrograph showing the region of the parent axon contiguous with both branches. There were notable differences between the two branches and the parent axon with regard to their content of unlabeled polymer. In the region of the parent axon just proximal to the branch point, 19% of the polymer was unlabeled. In the larger branch, virtually all of the polymer was labeled. Notably, in regions along the length of the smaller branch, 40–50% of the polymer was unlabeled. Thus, with this methodology, no MT transport was detectable in the larger branch, but significant MT transport was detectable in the smaller branch.

The starting lengths, amounts of axon growth, and percentages of unlabeled polymer scored in discrete regions at various points along the lengths of all 19 axons examined are shown schematically in Fig. 6. Each neuron is labeled with a Roman numeral, and individual axons from the same neuron are given separate letters. The axon shown in Fig. 3 is labeled IX-B in Fig. 5. The axon shown

in Fig. 4 is labeled IV-A in Fig. 6. The axon shown in Fig. 5 is labeled III-B in Fig. 6. Axons IV-C and IV-D were already-formed branches from a parent axon, as were axons VIII-C and VIII-D. Five of the 19 axons contained no detectable unlabeled polymer whatsoever within the sites we examined in their newly grown regions. An additional nine contained no unlabeled polymer directly behind their growth cones but contained unlabeled polymer (6–50%) at more proximal sites within their newly grown regions. The remaining five axons contained unlabeled polymer (1–28%) throughout their newly grown regions, including sites directly behind their growth cones. Together, these data demonstrate that MT assembly and/or turnover is active in growing axons and also that preassembled MTs are transported into newly grown regions of the axon. This transport is detectable in some but not all axons using our methodology.

Discussion

The goal of the present study was to use a high resolution approach to visualize the contributions of MT assembly
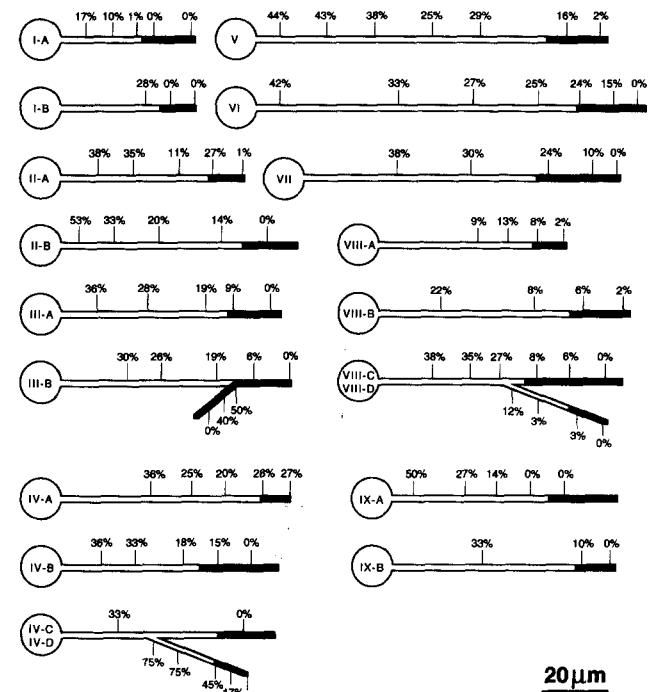

Figure 6. Summary of data from all axons examined. The starting lengths, amounts of axon growth, and percentages of unlabeled polymer scored at various points along the lengths of all 19 axons examined are shown schematically. Each neuron is labeled with a Roman numeral, and individual axons from the same neuron are given separate letters. Five of the 19 axons contained no detectable unlabeled polymer whatsoever in their newly grown regions. An additional nine contained no unlabeled polymer directly behind their growth cones but contained unlabeled polymer (6–50%) at other sites within their newly grown regions. The remaining five axons contained unlabeled polymer (1–28%) throughout their newly grown regions, including sites directly behind their growth cones. All percentages are indices calculated from measurements obtained from 4-μm regions of the axon (see Materials and Methods). Bar, 20 μm.

and transport during axon growth, and to do so in neurons that were not subjected to drugs or other experimental perturbations. Our strategy was to introduce biotinylated tubulin into cultured sympathetic neurons after the outgrowth of short axons, permit the axon to grow longer, and then use immunoelectron microscopy to visualize the distribution of labeled and unlabeled polymer. We reasoned that the labeled polymer assembled or turned over its subunits during the time frame of the experiment, while unlabeled polymer did not. Therefore, the presence of any unlabeled polymer in the newly grown region of the axon is indicative of MT transport. Our analyses demonstrate both labeled and unlabeled polymer throughout the axon, including the newly grown region, thus documenting that both MT assembly and transport occur during axon growth.

The most apparent feature of the electron micrographs is that the majority of the MT profiles both in the older and the newly grown regions of the axon incorporated biotinylated tubulin over the 40-min time frame of the experiment. These results show that a great deal of MT assembly and/or subunit turnover occurs within the growing axons of cultured sympathetic neurons. In recent light microscopic analyses, Li and Black (1996) reached the same conclusion and showed that these axons contain at least two classes of MT polymer that differ in their dynamic properties (Li and Black, 1996). The more labile class turns over with a half-time of ~1.3 h, while the more stable class turns over a half-time of ~3.3 h (Li and Black, 1996). Thus, in our studies, we would expect about half of the labile polymer but only trace amounts of the stable polymer to contain biotinylated tubulin 40 min after injection. An additional complication is the fact that the stable and labile classes of polymer exist in the form of distinct domains on individual MTs in the axon. The stable domain is situated at the minus end of the MT, and the labile domain assembles directly from its plus end (Baas and Black, 1990; Brown et al., 1993). Because axonal MTs are oriented with their plus ends distal to the cell body, the most distal portion of the axon is enriched in the more labile class of polymer (Baas and Black, 1990; Ahmad et al., 1993). Thus, it is not at all surprising that most of the polymer in the distal region of the axon incorporates biotinylated tubulin over 40 min, and that unlabeled polymer is most readily detected in most axons in the more proximal few microns of their newly grown regions. In considering our results, it is important to realize that high levels of labeled polymer would be enriched distally regardless of whether or not the polymer also underwent transport during that period of time. That is, the incorporation of biotinylated tubulin into a MT does not mean that it was not also transported as it assembled or turned over its subunits. Thus, the levels of unlabeled polymer in the newly grown region of the axon represent a minimum measurement of the amount of moving polymer, and quite likely underestimate the actual contribution of MT transport during the time frame of the experiment.

The idea that tubulin is transported in the form of assembled polymer was originally proposed on the basis of kinetic analyses (for review see Lasek, 1986). These studies demonstrated that tubulin is actively transported at a relatively constant rate, as a relatively coherent wave, and in a form that is not lost under conditions that remove free tubulin subunits. More recent support for MT transport has been provided by pharmacologic studies showing that when MT dynamics are suppressed, MTs gradually empty from the cell body and accumulate in growing axons (Baas and Ahmad, 1993; Smith, 1994; Ahmad and Baas, 1995). An alternate conclusion, that axonal MTs are stationary, has been reached by certain authors on the basis of light microscopic analyses on living neurons. Most of these studies, using photobleaching or photoactivation to make a discrete mark across the axonal MT array, failed to reveal movement of the mark (see, for example, Okabe and Hirokawa, 1989; Lim et al., 1990; Takeda et al., 1995; Sabry et al, 1995). The meaning of these results has been equivocal, however, in light of the potential for photodamage inhibiting MT movements (Keith and Farmer, 1993), as well as factors relating to the normal biology of the system. For example, MT transport may be less active in relatively short axons in which simple diffusion could supply sufficient tubulin subunits for axon growth. Interestingly, MT transport is most readily detected in live-cell studies on Xenopus axons (Reinsch et al., 1991), the only type of axon studied to date with this approach that grows more rapidly than the rate at which diffusion could supply sufficient tubulin subunits for local assembly to suffice (see Sabry et al., 1995).

In addition to documenting MT transport, our high resolution results provide additional insights into why MT transport may be difficult to detect in live-cell light microscopic analyses. It has been estimated that >10–20% of the polymer would have to be moving in order for the movement to be detected by the photobleach/photoactivation method (Lim et al., 1990; Sabry et al., 1995). This limitation is further complicated by the fact that highly asynchronous movements could throw the marked regions of different MTs out of alignment, thus rendering MT transport even more difficult to detect (Joshi and Baas, 1993). Our electron micrographs show that the alignment of several unlabeled MTs is quite rare, and hence suggest that such asynchrony exists. In addition, our studies dramatically illustrate how the rapid exchange of marked and unmarked subunits could obscure potential MT movements, further diminishing the numbers of MTs whose transport could be detected by the live-cell approach. It is possible that the Xenopus system mentioned above may have more stable and/or more tightly associated MTs, rendering their transport more detectable.

An inherent disadvantage of our approach is that we are unable to determine the actual levels of polymer that are moving. Therefore, we cannot resolve whether or not variations in the levels of unlabeled polymer in the newly grown regions of different axons reflect differences in the degree to which MTs were transported. Another possibility is that these variations simply reflect the proportions of polymer that did or did not incorporate the probe during the 40-min time period. Some support for this latter possibility derives from the fact that we could not predict the levels of unlabeled polymer on the basis of either the starting length of the axon or the degree to which it elongated during the 40 min. Worth special attention with regard to this issue was one unusual axon in which the growth cone underwent a very asymmetric bifurcation. The larger branch was essentially the continuation of the parent axon,

while the smaller branch grew off to one side, somewhat akin to a collateral branch. The larger branch contained virtually no unlabeled polymer, while almost half of the polymer in the smaller branch was unlabeled. In fact, the smaller branch contained the highest levels of unlabeled polymer in any newly grown axon region that we examined. These results suggest that MT transport may be especially active during the formation of a side branch, or alternatively, that the MTs transported into a side branch may be enriched in the more stable class of polymer. Previous studies on cultured hippocampal neurons are consistent with the latter possibility, indicating that MTs within newly forming collateral branches are more stable than those extending into the terminal growth cone (Yu et al., 1994). These studies, using tyrosinated tubulin as an indirect marker of newly assembled polymer, showed that the ratio of tyrosinated to total tubulin is notably higher within the polymer in the distal region of the axon compared to the main shaft, but is essentially the same within the main shaft and newly forming branches.

In conclusion, the high resolution afforded by our strategy clearly demonstrates that MT transport is a reality and also illustrates that MT transport and assembly events occur concomitantly during axon growth. These findings support a model for the elaboration of the axonal MT array based on both types of MT behavior. Our results provide no evidence for the active transport of tubulin in the form of free subunits or oligomers, but additional studies will be required to directly address these potential transport forms of tubulin. In addition, new strategies will be required to reveal MT transport within the axons of living neurons and to elucidate the interplay between the transport of axonal MTs, their dynamic properties, and the specific behaviors that the axon undergoes as it grows.

Note added in proof. In a recent study, fluorescent stable microtubule fragments were injected into living squid axons, and these fragments were observed to move anterogradely down the axon at the rate of slow transport (Terasaki, M., A. Schmidek, J.A. Galbraith, P.E. Gallant, and T.S. Reese. 1995. Transport of cytoskeletal elements in the squid giant axon. *Proc. Natl. Acad. Sci. USA.* 92: 11500–11503).

References

Ahmad, F.J., and P.W. Baas. 1995. Microtubules released from the neuronal centrosome are transported into the axon. *J. Cell Sci.* 108:2761–2769.

Ahmad, F.J., T.P. Pienkowski, and P.W. Baas. 1993. Regional differences in microtubule dynamics in the axon. *J. Neurosci.* 13:856–866.

Baas, P.W., and F.J. Ahmad. 1992. The plus ends of stable microtubules are the exclusive nucleating structures for microtubules in the axon. *J. Cell Biol.* 116: 1231–1241.

Baas, P.W., and F.J. Ahmad. 1993. The transport properties of axonal microtubules establish their polarity orientation. *J. Cell Biol.* 120:1427–1437.

Baas, P.W., and M.M. Black. 1990. Individual microtubules in the axon consist of domains that differ in both composition and stability. *J. Cell Biol.* 111: 495–509.

Baas, P.W., and W. Yu. 1996. Establishing the microtubule arrays of the neuron. *Mol. Neurobiol.* In press.

Bamburg, J.R., D. Bray, and K. Chapman. 1986. Assembly of microtubules at the tip of growing axons. *Nature (Lond.).* 321:788–790.

Brown, A., Y. Li, T. Slaughter, and M.M. Black. 1993. Composite microtubules of the axon: quantitative analysis of tyrosinated and acetylated α-tubulin along axonal microtubules. *J. Cell Biol.* 119:867–882.

Joshi, H.C., and P.W. Baas. 1993. A new perspective on microtubules and axon growth. *J. Cell Biol.* 121:1191–1196.

Keith, C., and M. Farmer. 1993. Microtubule behavior in PC12 neurites: variable results obtained with photobleach technology. *Cell Motil. Cytoskeleton.* 25:345–357.

Lasek, R.J. 1986. Polymer sliding in axons. *J. Cell Sci. Suppl.* 5:161–179.

Li, Y., and M.M. Black. 1996. Microtubule assembly and turnover in growing axons. *J. Neurosci.* 16:531–544.

Lim, S.-S., K.J. Edson, P.C. Letourneau, and G.G. Borisy. 1990. A test of microtubule translocation during neurite elongation. *J. Cell Biol.* 111:123–130.

Okabe, S., and N. Hirokawa. 1988. Microtubule dynamics in nerve cells: analysis using microinjection of biotinylated tubulin into PC12 cells. *J. Cell Biol.* 107:651–664.

Okabe, S., and N. Hirokawa. 1989. Turnover of fluorescently labeled tubulin and actin in the axon. *Nature (Lond.).* 338:662–664.

Reinsch, S.S., T.J. Mitchison, and M.W. Kirschner. 1991. Microtubule polymer assembly and transport during axonal elongation. *J. Cell Biol.* 115:365–380.

Sabry, J., T.P. O'Connor, and M.W. Kirschner. 1995. Axonal transport of tubulin in Ti1 pioneer neurons in situ. *Neuron.* 14:1247–1256.

Schulze, E., and M. Kirschner. 1986. Microtubule dynamics in interphase cells. *J. Cell Biol.* 102:1020–1031.

Smith, C.L. 1994. The initiation of neurite outgrowth by sympathetic neurons grown in vitro does not depend on assembly of microtubules. *J. Cell Biol.* 127:1407–1418.

Takeda, S., T. Funakoshi, and N. Hirokawa. 1995. Tubulin dynamics in neuronal axons of living zebrafish embryos. *Neuron.* 14:1257–1264.

Webster, D.R., and G.G. Borisy. 1989. Microtubules are acetylated in domains that turn over slowly. *J. Cell Sci.* 92:57–65.

Yu, W., and P.W. Baas. 1995. The growth of the axon is not dependent upon net microtubule assembly at its distal tip. *J. Neurosci.* 15:6827–6833.

Yu, W., F.J. Ahmad, and P.W. Baas. 1994. Microtubule fragmentation and partitioning in the axon during collateral branch formation. *J. Neurosci.* 14: 5872–5884.